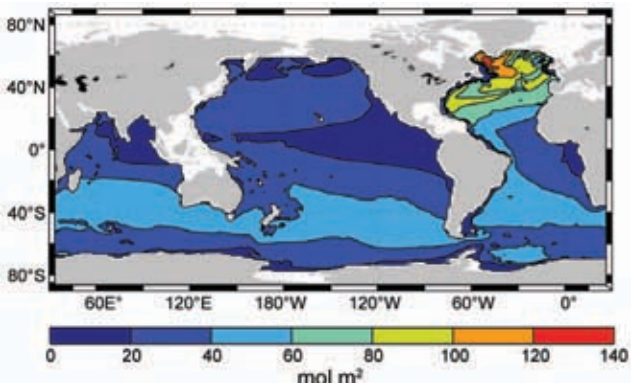

Fig. 3.30. Map of the column inventory of anthropogenic CO_2 in 2008. Adapted from Khatiwala et al. 2009.

One advantage of the Khatiwala estimates is the ability to examine the changes in ocean carbon storage over time. For example, these estimates suggest that the annual rate of ocean carbon storage has grown every year since the late 1700s, but the rate increased sharply in the 1950s in response to faster growth in atmospheric CO_2. In recent decades, however, the rate of increase in ocean carbon storage has not been able to keep pace with the atmospheric growth rate. The percentage of annual anthropogenic CO_2 emissions stored in the ocean in 2008 was as much as 10% smaller than the percentages of the previous decade, although significant uncertainties remain which preclude a more definitive statement. The rapid growth in emissions over the past 10 years relative to the previous decade is one important factor in the reduction in the ocean's relative uptake of anthropogenic CO_2 emissions. Another key factor is the decreasing ability of the seawater to store the CO_2 as dissolved inorganic carbon. This reduced capacity is a natural and predictable consequence of ocean carbon chemistry that, in the absence of changes in large-scale circulation or ocean biology, will become more significant with time (Egleston et al. 2010). By comparing the Khatiwala estimates at the time and location of the repeat hydrography cruises the measured ocean carbon changes can be used to validate the C_{ant} estimates and monitor for changes in the natural ocean carbon cycle not constrained by the Khatiwala technique.

j. Global ocean phytoplankton—R. T. O'Malley, M. J. Behrenfeld, D. A. Siegel, and S. Maritorena

Photosynthesis by the free-floating, single-celled phytoplankton of the upper-sunlit "photic" layer of the global ocean is the overwhelmingly dominant source of organic matter fueling marine ecosystems. Phytoplankton contribute roughly half of the annual biospheric (i.e., terrestrial and aquatic) net primary production (NPP; gross photosynthesis minus plant respiration), and their photosynthetic carbon fixation is the primary conduit through which atmospheric CO_2 is transferred into the ocean's organic carbon pools. These tiny suspended ocean "plants" play a vital role on the Earth's biogeochemical cycles, and are the very base of the oceanic food chain. The productivity of phytoplankton depends on the availability of sunlight, macronutrients (e.g., nitrogen, phosphorous), and micronutrients (e.g., iron), and thus is sensitive to changes in these resources.

Since 1997, a continuous record of global satellite ocean color observations has been available, allowing the investigation of relationships between ocean environmental conditions and plankton ecology (e.g., McClain 2009; Behrenfeld 2010). The ecosystem property most often derived from ocean color data is surface chlorophyll concentration (Chl_{sat}) (Fig. 3.31a). Chl_{sat} provides an estimate of phytoplankton pigment concentration throughout the upper ocean mixed layer and its variability reflects the combined influence of phytoplankton standing stock (biomass) changes and physiological responses to prevailing light and nutrient levels. Values of Chl_{sat} span three orders of magnitude globally (roughly 0.03 to >30 mg m^{-3}) with a distribution closely aligned with primary ocean circulation features. Thus, high Chl_{sat} is found in regions of seasonal deep mixing (e.g., North Atlantic) and upwelling (e.g., Equatorial Pacific, west coast of Africa), while low values are found in permanently stratified ocean regions, particularly the low-nutrient central ocean gyres (white contours in Fig. 3.31a).

Climate-scale analyses require both *continuity* and *consistency* in the underlying observations for correct assessments of change. Unfortunately, these attributes are not satisfied for the most recent period of satellite ocean color measurements. Starting in 2008 and after more than a decade of continuous coverage, observations from the Sea-viewing Wide-Field-of-view Sensor (SeaWiFS) became intermittent due to issues with the spacecraft and telemetry. No SeaWiFS imagery was collected for the first 88 days of 2008 and, over the whole year, only 31 of 46 possible eight-day composite images could be processed. Data gaps also exist for 2009, with only 34 valid eight-day composites available over the year. Thus, 30% of the SeaWiFS record is missing for 2008/09 and only one-third of the eight-day composites are temporally matched for the two years. This lack of continuity strongly restricts an interannual comparison. Fortunately, half of the

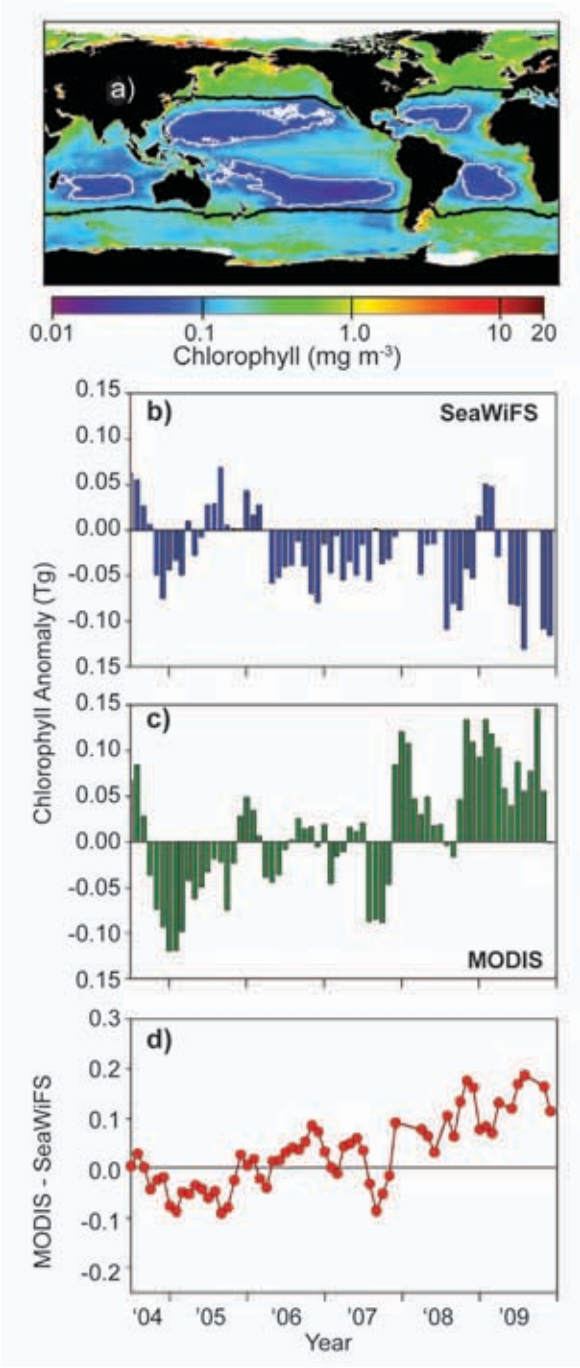

Fig. 3.31. (a) Average MODIS-*Aqua* Chl_{sat} for 2009. Heavy black lines indicate where average SST=15°C, which is used herein to distinguish the permanently stratified ocean from northern and southern strongly-seasonal regions. White contours identify central ocean gyres, as defined by average Chl_{sat} values of 0.07 mg m^{-3} (see also McClain et al. 2004; Polovina et al. 2008; and Henson et al. 2009). (b) Mid-2004 through 2009 monthly chlorophyll anomalies for the SeaWiFS (data from latest reprocessing: r2009.1). (c) Mid-2004 through 2009 monthly chlorophyll anomalies for the MODIS-*Aqua*. (d) MODIS-SeaWiFS anomaly difference. Data in (b), (c), and (d) are for the permanently stratified oceans (average SST>15°C).

coverage common to both years occurred at the end of the calendar year, providing two months of continuous coverage of the El Niño event developing over the latter half of 2009 (Chapter 4a).

Consistency between available U.S. ocean color datasets is also a problem. In the *State of Climate in 2008* report, we noted a relatively constant offset between the SeaWiFS Chl_{sat} record and concurrent data from the MODerate resolution Imaging Spectrometer (MODIS) on the *Aqua* platform. Accordingly, we found reasonable agreement between temporal chlorophyll anomalies for the two sensors (Behrenfeld et al. 2009) [as in the current report, anomalies were calculated as the difference between an observed value for a given month and the average value for that month over a sensor's full record (e.g., 1997–2009 for the SeaWiFS)]. Unfortunately, discrepancies between Chl_{sat} anomalies for the SeaWiFS (Fig. 3.31b) and MODIS-*Aqua* (Fig. 3.31c) increased during 2009, such that a simple offset correction is no longer adequate. The temporal evolution of this intersensor inconsistency is clearly revealed in the MODIS-SeaWiFS anomaly difference for the period 2004 to 2009 (Fig. 3.31d). While this issue of inconsistency has limited the current analysis of Chl_{sat} changes to SeaWiFS data only, it is important to note that the full MODIS-*Aqua* dataset is currently being reprocessed by the NASA Ocean Biology Processing Group and preliminary comparisons between the SeaWiFS and reprocessed MODIS-*Aqua* scenes look excellent (see http://oceancolor.gsfc.nasa.gov/REPROCESSING/R2009/ for more details). Nevertheless, this experience emphasizes the critical importance of monitoring and updating ocean color sensor calibrations/algorithms and conducting periodic data reprocessing to achieve data quality levels adequate for satellite-based global climate studies.

To investigate changes in global ocean chlorophyll stocks during 2009, available SeaWiFS data were analyzed following methodologies originally described in Behrenfeld et al. (2006) and employed in our two previous *State of the Climate* reports (Behrenfeld et al. 2008b, 2009). Chl_{sat} data (mg m^{-3}) were integrated to the 1% light level to calculate "photic zone" chlorophyll concentrations (ΣChl). For analysis of chlorophyll anomaly trends, global data were binned into three broad regions: the permanently stratified ocean (approximated as those waters with annual average SST > 15°C), strongly seasonal high-latitude northern waters (average SST < 15°C), and strongly-seasonal high-latitude southern waters (average SST < 15°C).

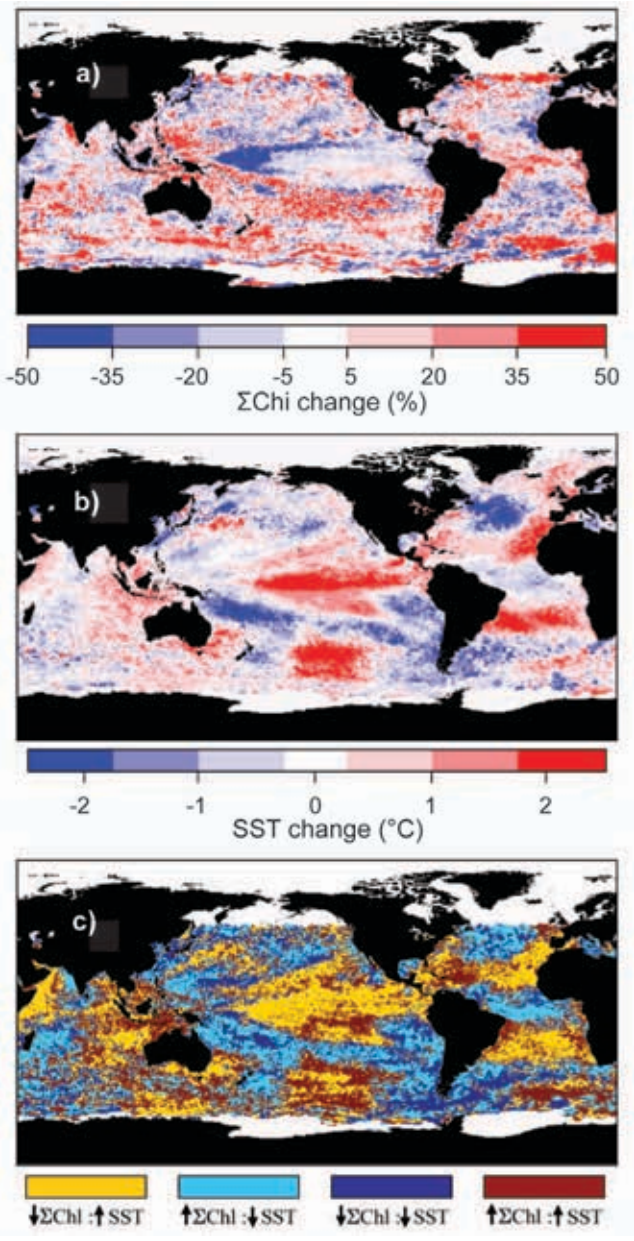

Fig. 3.32. (a) Percent change in November–December average depth-integrated chlorophyll (∑Chl) between 2009 and 2008. (b) Absolute change in November–December average SST between 2009 and 2008. (c) State-space comparison between ∑Chl and SST (from panels a and b). Yellow = increasing SST, decreasing ∑Chl. Red = increasing SST, increasing ∑Chl. Dark blue = decreasing SST, decreasing ∑Chl. Light blue = decreasing SST, increasing ∑Chl.

For each region, ΣChl data (mg m^{-2}) were summed over surface area to give total chlorophyll stocks in units of teragrams (Tg = 10^{12} g).

Spatiotemporal variations in Chl_{sat} are driven by variability in phytoplankton biomass, nutrient stress, and light acclimation (i.e., photoacclimation), all of which are linked to physical changes within the surface mixed layer. Changes in SST provide one index of this variability in the physical environment and can be compared globally to changes in Chl_{sat} (Behrenfeld et al. 2006, 2008a, 2009). The relationship between phytoplankton chlorophyll and SST changes for the 2008 to 2009 period is best illustrated over the November–December period corresponding to the strengthening of the 2009 El Niño (Fig. 3.32). For this period, expansive and spatially coherent regions are seen of increasing and decreasing ΣChl (Fig. 3.32a). In particular, ΣChl decreased over much of the equatorial Pacific in response to lower nutrient levels associated with reduced rates of upwelling. In contrast, significant increases in ΣChl are found in the western tropical Pacific, the south Pacific and Indian subtropical gyres and the equatorial Atlantic Ocean (Fig. 3.32a). These changes in ΣChl correspond to similar spatial patterns in SST changes (Fig. 3.32b), again illustrating the close link between ocean biology and their physical environment.

Overall for the stratified oceans, 63% of the pixels with increased SST for November–December 2009 also exhibited decreased in ΣChl (yellow pixels in Fig. 3.32c). Likewise, 60% of the pixels with decreased SST corresponded to increased ΣChl (light blue pixels in Fig. 3.32c). This dominant inverse relationship between SST changes and ΣChl changes is consistent with surface-ocean warming (cooling) being associated with decreasing (increasing) vertical nutrient transport and increasing (decreasing) mixed-layer light levels, with light and nutrient changes driving changes in both phytoplankton cellular pigment levels and biomass.

Relationships between global chlorophyll fields and SST illustrated in Fig. 3.32 are seen at a much broader level when cast against the full 12-year SeaWiFS record for the three regions described above. For this comparison, monthly anomalies in regional SeaWiFS chlorophyll stocks were matched to SST anomalies constructed by merging MODIS-*Aqua* SST4 data (2003–09) and AVHRR (quality 5–8) SST data (1997–2003) (regionally-integrated SST data have units of °C m^2 and are hereafter referred to as "thermal anomalies"). Once again, an overall inverse relationship emerges at the regional scale for the full SeaWiFS record [Fig. 3.33 – note that the thermal anomaly axes are inverted (i.e., cooling at top, warming at bottom)]. Indeed, the newly reprocessed SeaWiFS data provides an even closer match between thermal anomalies and chlorophyll anomalies than previously reported (e.g., compare to Behrenfeld et al. 2009). At high-northern

latitudes, chlorophyll and thermal oscillations were relatively constrained between 1997 and 2006 and then showed significantly stronger variability (Fig. 3.33a). As in previous reports (Behrenfeld et al. 2008b, 2009), chlorophyll and thermal anomalies exhibited the largest temporal changes in the permanently stratified, lower-latitude oceans (Fig. 3.33b – note different axis scaling), with a large initial trend of increasing chlorophyll and decreasing temperature associated with the 1997–99 El Niño (Behrenfeld et al. 2006). From 1999 onward, an overall progressive decrease in chlorophyll is observed and coincident with a general increasing trend in ocean-surface temperature (Fig. 3.33b). At high southern latitudes, temporal trends in chlorophyll and thermal anomalies are weaker (Fig. 3.33c).

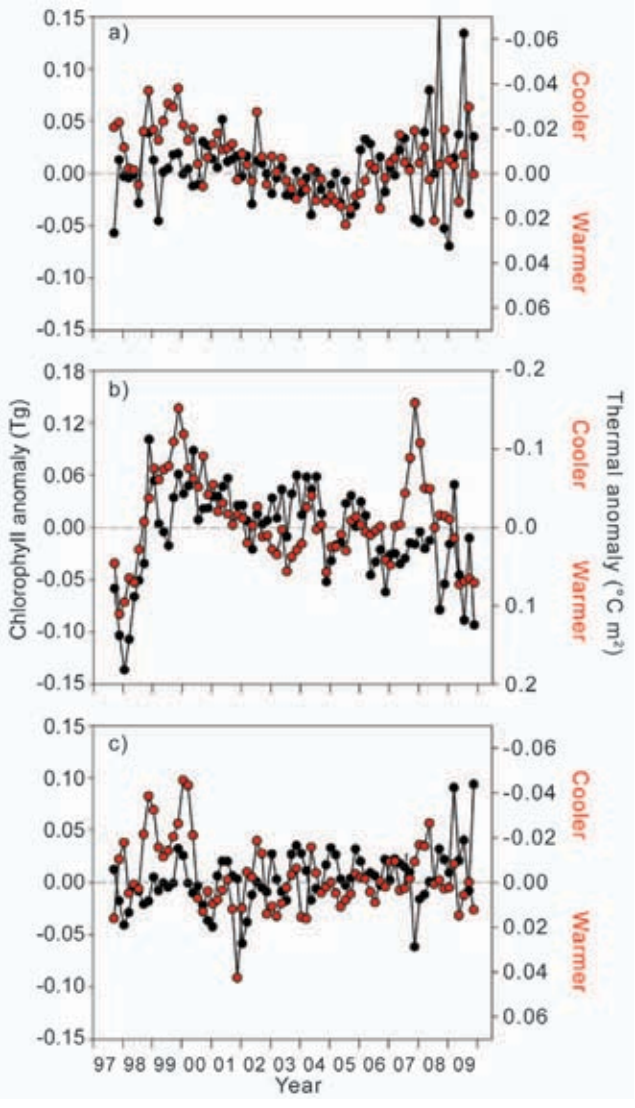

Fig. 3.33. Twelve-year record of monthly SeaWiFS chlorophyll anomalies (black symbols, left axis, Tg) and monthly AVHRR/MODIS thermal anomalies (red symbols, right axis, °C m^2 x10^{15}). (a) Northern waters with average SST < 15°C. (b) Permanently stratified waters with average SST > 15°C. (c) Southern waters with average SST < 15°C. See Fig. 3.31a for location of each region. Horizontal dashed line in each panel = 0. Thermal anomaly axes (right) are inverted to illustrate the general inverse relationship with chlorophyll anomalies and thermal anomalies. Note that the use of thermal anomalies in this figure differs from Behrenfeld et al. 2008b and 2009. This change was made to preserve identical processing with the chlorophyll signal.

While comparisons of surface chlorophyll and temperature data illustrate the strong dependencies of biology on physical forcings, it is important to recognize that the underpinnings of such relationships are correlative not causative. For each region, the full range in thermal anomalies represents an average change in SST that barely spans 1°C. The direct physiological consequences (e.g., enzymatic reaction rates) of such minute temperature changes are negligible. Thus, correlations between SST and chlorophyll anomalies emerge because SST acts as a surrogate for other environmental factors that covary with SST and directly impact phytoplankton chlorophyll levels. Two such factors are nutrient supply and mixed-layer light levels. In general, surface-layer warming is associated with stronger surface-layer stratification and shallower mixing depths, which in turn increase average mixed-layer phytoplankton light exposure and can hamper vertical nutrient exchange (Behrenfeld et al. 2005; Siegel et al. 2005). Decreased nutrient availability suppresses phytoplankton cellular chlorophyll levels and can diminish phytoplankton biomass. Likewise, acclimation to enhanced mixed-layer light exposure entails reductions in cellular chlorophyll. Changes in seasonal surface mixing cycles can also influence chlorophyll levels by altering predator–prey interactions and thereby phytoplankton biomass and species composition (Behrenfeld 2010). Thus, it is the correlation between SST and the summed expression of these, and other, direct forcings that gives rise to inverse chlorophyll–SST relationships. It is essential that these *functional* relationships be carefully considered when interpreting observed global changes in satellite chlorophyll fields and when projecting observed changes to longer time-scale trends.